Electronic structure and electron-positron correlation effects in Mg

1990 J. Phys.: Condens. Matter 2 9927

(http://iopscience.iop.org/0953-8984/2/49/017)

J. Phys.: Condens. Matter **2** (1990) 9927–9939. Printed in the UK

Electronic structure and electron–positron correlation effects in Mg

G Kontrym-Sznajd and J Majsnerowski
W Trzebiatowski Institute of Low Temperature and Structure Research, Polish Academy of Sciences, 50–950 Wroclaw 2, PO Box 997, Poland

Received 15 January 1990, in final form 18 June 1990

Abstract. A reconstruction of 3D electron–positron densities from 2D ACPAR experimental spectra for Mg was performed using Cormack's method and compared with theoretical results. In theoretical calculations the LMTO band structure method was applied. Many-body effects have been incorporated in a local density approximation both for valence and core electrons.

These results lead to improved agreement between theory and experiment in comparison to the independent particle model. For the first time an over-enhancement of the higher momentum components was obtained both theoretically and experimentally.

1. Introduction

The measurement of the angular correlation of positron annihilation radiation (ACPAR) has proved to be a useful technique for studying the electronic structure of solids [1, 2]. Using 2D position-sensitive γ-ray detectors yields 2D ACPAR spectra:

$$N(p_x, p_y) = \int \rho(\boldsymbol{p})\, \mathrm{d}p_z \tag{1}$$

where $\rho(\boldsymbol{p})$ is the electron–positron (e–p) momentum density. The function $\rho(\boldsymbol{p})$ contains information about the Fermi surface (FS) and the nature of the positron and electron wavefunctions as well as about many-particle effects.

The presence of the positron in a metal does not change the Fermi momentum [3] (as the positron is thermalized before annihilation [4]) but, unfortunately, deforms electronic wavefunctions (the electron density is enhanced at the positron position). This enhancement is described by the effective enhancement factor (EF) [5] defined as the ratio of the total density $\rho(\boldsymbol{p})$ to the density calculated within the independent particle model (IPM):

$$\tilde{\varepsilon}(\boldsymbol{p}) = \rho(\boldsymbol{p})/\rho^{\mathrm{IPM}}(\boldsymbol{p}). \tag{2}$$

Here $\tilde{\varepsilon}(\boldsymbol{p})$, which depends on the enhancements of various electronic states, is the only quantity that can be essentially extracted from the experiment as far as information about the e–p interaction is concerned.

The purpose of this paper is to interpret 2D ACPAR experimental spectra for Mg [6]. For that the reconstruction of $\rho(\boldsymbol{p})$ was performed by applying Cormack's method [7]

0953-8984/90/499927 + 13 $03.50

as described in [8]. Theoretical densities were computed both within IPM and taking into account the e–p correlation in the local density approximation [9].

The experimental spectra for Mg were obtained by Walters and co-workers [6] on the UEA (University of East Anglia) 2D angular correlation spectrometer with a resolution of the order 0.7 mrad (1 mrad = 0.137 au). The measurement was performed for two crystal orientations: with direction of integration p_z (in equation 1) along $[10\bar{1}0]$ ($N_{\Gamma M}$) and $[11\bar{2}0]$ ($N_{\Gamma K}$) and at a temperature of 120 K. The total counts at peak were of the order 70 000.

Mg is a simple HCP metal with two s electrons per atom. Although its electronic structure is known, information on the momentum dependence of the e–p density $\rho(\boldsymbol{p})$ and the EF is scarce. As far as we know, there is no information about the $\tilde{\varepsilon}(\boldsymbol{p})$ in Mg, both for the core electrons and the higher momentum components (HMC) of the valence electrons.

On the basis of ACPAR data the authors of the papers [4, 6, 10, 11] determined isotropic effective EFs for the valence electrons inside the FS in Mg. Shiotani and co-workers [11] also obtained core enhancement factors which they considered to be momentum independent as well as absolute values for the enhancement of the valence and core electrons determined from the total annihilation rates. Moreover, they observed the anisotropy at high momenta related to the anisotropic contribution of the HMC.

In this paper we present the results obtained for the e–p density $\rho(\boldsymbol{p})$ both inside the Fermi surface and in the region of higher momenta (core and HMC). The momentum dependent anisotropic EF $\tilde{\varepsilon}(\boldsymbol{p})$ for the valence electrons, $\tilde{\varepsilon}^{v}(\boldsymbol{p})$, and the isotropic one for the core electrons, $\tilde{\varepsilon}^{c}(\boldsymbol{p})$, are determined. It follows from our theoretical results that the contribution from the third band in $[10\bar{1}0]$ direction (obtained in IPM) is over-enhanced, i.e. $\tilde{\varepsilon}_l(\boldsymbol{k}+\boldsymbol{G}) > \varepsilon_l(\boldsymbol{k})$ where $\boldsymbol{k}$ and $\boldsymbol{G}$ denote the momentum in the reduced zone scheme of the lth band and a reciprocal lattice vector, respectively. The densities $\rho(\boldsymbol{p})$ reconstructed from the experimental data exhibit a similar effect.

As far as FS dimensions obtained from the positron annihilation experiment are concerned, Kubica and Stewart [4] measured the 1D ACPAR curve with good equipment resolution and obtained with high accuracy $p_F[0001] = 0.725 \pm 0.001$ au (where p_F denotes the Fermi momentum). Shiotani and co-workers [11] observed a reduction of butterflies (FS elements in the third band around the L point of the Brillouin zone) giving their dimensions in the [0001] direction. On the basis of our results, which were obtained from the reconstruction of $\rho(\boldsymbol{p})$, we observed reductions in the size of the butterflies as well as the holes around the H point in the first and second Brillouin zones.

The band structure of Mg, which is a starting point in our theoretical calculations, has been computed by Daniuk and co-workers [12].

2. Method

2.1. Theoretical calculations

The LMTO method in the atomic sphere approximation was employed to calculate the band structure [12] and crystal wavefunctions for itinerant electrons (the details of the applied method are presented in [13–15]). The band structure calculations were performed self-consistently using the exchange and correlation contribution to the

potential in non-spin-polarized form given by Hedin and co-workers [16]. The wavefunctions were calculated semi-relativistically including all relativistic terms except the spin–orbit coupling.

The positron wavefunction can be calculated in the same way using the Coulomb part of the electron potential with the opposite sign. However, taking into account the fact that the positron is thermalized, only the lowest state E^+ at the Γ point ($\boldsymbol{k} = 0$) is the state of interest. Since it has mainly $l = 0$ character, the positron wavefunction can be described (to a good approximation) by the radial solution $R(E^+, r)$ of the Schrödinger equation for the energy E^+. Thus, we used the positron wavefunction in the following form:

$$\Psi_+(r) = (4\pi)^{-1/2} R(E^+, r). \tag{3}$$

The IPM e–p pair momentum distribution was calculated using the following formula:

$$\rho^{\mathrm{IPM}}(\boldsymbol{p}) = \sum_{k,n}^{\mathrm{occ}} \left| \int \Psi_{k,n}(\boldsymbol{r}) \Psi_+(\boldsymbol{r}) \exp(-\mathrm{i}\boldsymbol{p}\cdot\boldsymbol{r})\, \mathrm{d}\boldsymbol{r} \right|^2 \tag{4}$$

where $\Psi_{k,n}(\boldsymbol{r})$ denotes the electron wavefunction in the nth band. In calculations of momentum densities, overlap corrections due to the overlapping sphere geometry (especially very important for the Umklapp processes) [17] were applied. Many-body e–p correlation effects were incorporated in the local density approximation proposed by Daniuk and co-workers [9]. The e–p pair momentum density was obtained according to the following formula:

$$\rho(\boldsymbol{p}) = \sum_{k,n}^{\mathrm{occ}} \left| \int \sqrt{\varepsilon(\boldsymbol{r})}\, \Psi_{k,n}(\boldsymbol{r}) \Psi_+(\boldsymbol{r}) \exp(-\mathrm{i}\boldsymbol{p}\cdot\boldsymbol{r})\, \mathrm{d}\boldsymbol{r} \right|^2 \tag{5}$$

where the function $\varepsilon(\boldsymbol{r}) = \varepsilon(\chi_{nk}(\boldsymbol{r}), r_s(\boldsymbol{r}))$ is the electron-gas EF $\varepsilon_{rs}(p)$ applied locally within the unit cell. The function

$$\chi_{nk}(\boldsymbol{r}) = (E_{nk} - V(\boldsymbol{r}))/(E_{\mathrm{F}} - V(\boldsymbol{r}))$$

represents the ratio of local kinetic energies. E_{nk} is the electron energy, E_{F} the Fermi energy, $V(\boldsymbol{r})$ is the crystal potential and $r_s(\boldsymbol{r})$ is the local electron density parameter [9].

In the case of the core electrons the density function $\rho_{c,nl}(p)$, corresponding to the nlth core shell, was determined according to the following formula [18]:

$$\rho_{c,nl}(p) = (2l+1) \left| \int \sqrt{\varepsilon(r)}\, R_{nl}(r) \Psi_+(r) j_l(pr) r^2\, \mathrm{d}r \right|^2 \tag{6}$$

where $R_{nl}(r)$ is the radial electron wavefunction and j_l is the spherical Bessel function. In both cases (i.e. in equations (5) and (6)) the EFs $\varepsilon_{r_s}(p)$ calculated within the Kahana formalism for an electron gas of various densities [19, 20] have been applied. It should be noted here that there are also other treatments of the e–p interaction in an electron gas, proposed by Lowy and Jackson (L–J) [21] and Arponen and Pajanne (A–P) [22]. However, within L–J's theory the momentum dependent EFs were calculated for $r_s \geqslant 3$ only [23], i.e. for densities greater than the ones occurring in Mg. As far as A–P's approach is concerned, the comparison of the theoretical EFs with experimental data shows that in simple metals (like Mg) the Kahana theory seems to be more adequate for describing the positron annihilation with valence electrons [20]. On the other hand, for

low r_s (i.e. for $r_s < 2$ which correspond to core densities) the values of the total annihilation rates calculated from Kahana and A–P theories are very similar [19]. Since these two theories give different EFs for valence electrons but very similar ones for core densities, we have chosen the EFs of Rubaszek and co-workers [19, 20]. Moreover, in the case of core electrons the momentum dependence of EFs was neglected [18], i.e. the energy-independent enhancement function $\varepsilon(\boldsymbol{r}) = \varepsilon(0, r_s(\boldsymbol{r}))$ was used in equation (6).

A similar approach was applied by Jarlborg and Singh [24] to determine the effective EF for d electrons in Ni. On the basis of the experimental results Singh and co-workers [25] found this enhancement to be a decreasing function of energy. The authors of [24] explained this fact theoretically, omitting the energy dependence of $\varepsilon(\boldsymbol{r})$ in (5). On the other hand, in the case of Ni the decrease with energy of the effective EF is also observed when the energy dependent EFs are applied in (5), as shown by Daniuk [26]. However, this effect was much weaker within the approach of [26] and vanished in the case of other d transition metals (as e.g. for Cr). Of course, only a detailed comparison of theoretical and experimental results for various metals could verify the validity of the above treatments and the obtained results.

2.2. Reconstruction method

In order to reconstruct the e–p densities $\rho(\boldsymbol{p})$ from the experimental 2D ACPAR data for Mg [6], we have applied the method proposed by Cormack [7]. In this method a 3D reconstruction is reduced to a set of 2D ones performed on the planes parallel to each other. In our case the reconstruction was performed on the planes perpendicular to the [0001] direction. The functions $N(p_x, p_y = \text{constant})$ and $\rho(\boldsymbol{p})$ were expanded into the cosine Fourier series with the radial coefficients $N_n(t)$ and $\rho_n(p)$, respectively (where, for the HCP structure, $n = 0, 6, 12$, etc [8a] and $t \equiv p_x$). In the case of two projections, the isotropic (N_0) and the first anisotropic (N_6) component of the projections were computed according to the following equations:

$$N_0(t) = (N_{\Gamma M} + N_{\Gamma K})/2 \qquad N_6(t) = (N_{\Gamma M} - N_{\Gamma K})/2. \tag{7}$$

The coefficients $\tilde{a}_0^m$ and $\tilde{a}_6^m$ of the expansion $N_0(t)$ and $N_6(t)$ into the series of the Chebyshev polynomials, respectively, were determined from the following equation [8c]:

$$N_n(t) = 2 \sum_{m=0}^{90} \tilde{a}_n^m \sin[(2m + 1)\psi] \tag{8}$$

where $t = \cos\psi$ corresponds to the unit system where $0 \leq t \leq 1$. Ninety values of $N_0(t)$ and $N_6(t)$ for $t = \cos(1°), \cos(2°), \ldots, \cos(90°)$ in equation (8) were used. Next, the density $\rho(\boldsymbol{p})$ was calculated according to the following equation:

$$\rho(p, \theta) = \sum_{n=0,6} \sum_{m=0}^{m_n} (n + 2m + 1) a_n^m R_n^m(p) \cos(n\theta) \tag{9}$$

where

$$a_n^m = \tilde{a}_n^{m+n/2}. \tag{10}$$

Equation (10) corresponds to the condition that the first $n/2$ coefficients $\tilde{a}_n^m$ are equal to zero, i.e. the lowest term in the expansion of $N_n(t)$ into the Chebyshev polynomial series is $\sin[(n + 1)\psi]$.

It has been demonstrated in [8b, 8c] that in the case of the HCP structure Cormack's method allows reproduction of the anisotropy of $\rho(\boldsymbol{p})$ (particularly the differences $\rho_{\Gamma K}(\boldsymbol{p}) - \rho_{\Gamma M}(\boldsymbol{p})$, as shown in [8c], p 237) even from two projections. The results shown here correspond to 2D ACPAR spectra reduced to the first quarter by taking the arithmetic average of four data sets. We present the results without smoothing of $\rho(\boldsymbol{p})$, i.e. all coefficients a_0^m ($m_0 = 89$) and a_6^m ($m_6 = 86$) estimated from equation (8) for $t = \cos(1°)$, $\cos(2°), \ldots, \cos(90°)$ were used in equation (9).

3. Results

3.1. Electron–positron pair momentum density

The e–p momentum densities $\rho(\boldsymbol{p})$ were reconstructed on the planes perpendicular to the [0001] direction and 0.367 mrad apart, which corresponds to the distance between the experimental points. Let $\boldsymbol{p}$ and $\tilde{\boldsymbol{p}}(|\tilde{p}| = (p^2 + p_y^2)^{1/2})$ denote the momentum on the plane $p_y \equiv p_{[0001]} =$ constant and in the space, respectively. The densities $\rho(\boldsymbol{p})$ on the plane P_1 (first plane for $p_y = 0.1835$ mrad) and on P_5 ($p_y = 1.6515$ mrad) have been presented in [8b, 28]. Since the greatest anisotropy of $\rho(\boldsymbol{p})$ for $\tilde{\boldsymbol{p}} > \tilde{\boldsymbol{p}}_F$ is observed on P_1 while for $\tilde{\boldsymbol{p}} \leqslant \tilde{\boldsymbol{p}}_F$ on P_5, our theoretical calculations were restricted to these two planes.

The agreement between theory and experiment is improved when the e–p interaction is included into the theoretical calculations. The application of the electron gas EF [19, 20] gives appropriate description of the momentum dependence of $\rho(\boldsymbol{p})$ for $p \leqslant 0.8p_F$ (figure 1(*a*)). Unfortunately, we are not able to compare the results for momenta close to p_F because of the smearing of $\rho(\boldsymbol{p})$ due to the equipment resolution. In order to do that it would be necessary to calculate $\rho(\boldsymbol{p})$ in the whole space, compute $N(p_x, p_y)$ taking into account the equipment resolution and, finally, perform a reconstruction of the theoretical spectra.

The results for $p > p_F$ are presented in figure 1(*b*), where both $\rho(\boldsymbol{p})$ in the ΓK direction and the difference between densities in ΓM and ΓK are drawn. Along the ΓK direction, where the HMC contribution of the first band is negligible, $\rho(\boldsymbol{p})$ depends mainly on the core density. Comparison of the values of the theoretical densities (0.0075 and 0.015 for IPM and correlated model, respectively) with those reconstructed from the experiment (0.016) shows that the EF for the core electrons is in accordance with the experiment.

Comparison between theory and experiment shows that on the P_1 plane the anisotropy of $\rho(\boldsymbol{p})$ is mainly due to the HMC contribution of the third band in the ΓM direction [8b, 28, 30]. Its maximum occurs for $p = 6.6$ mrad (figure 1(*b*)). This is in good agreement with the value $p \simeq 6.75$ mrad derived from experiment (a similar behaviour of $\rho(\boldsymbol{p})$ has been observed by Rozenfeld and Chabik [31]). As will be discussed in more detail in the next section, the application of the local density enhancement leads to an over-enhancement of the HMC in the ΓM direction. Quantitative comparison of the differences between $\rho_{\Gamma M}$ and $\rho_{\Gamma K}$ (figure 1(*b*)) shows that this effect is stronger in the case of the experimental data. Taking into account that the experiment was carried out at 120 K, where the HMC contribution should be reduced [32, 33], it seems that the reconstructed densities confirm the over-enhancement effect obtained theoretically.

With respect to the behaviour of $\rho(\boldsymbol{p})$ on the P_5 plane (figure 2), the difference $\Delta\tilde{\boldsymbol{p}}_F$ between the Fermi momentum in $[11\bar{2}0]$ and $[10\bar{1}0]$ directions obtained theoretically is equal to 0.06 mrad. This corresponds to the reduction both of the first zone holes around

the H point in the ΓK direction ($\simeq$0.03 mrad) and the butterflies in the ΓM direction ($\simeq$ 0.03 mrad) with respect to the free-electron FS. The anisotropy of the FS reproduced from 2D ACPAR data seems to be much greater, giving $\Delta\tilde{p}_F$ equal to 0.11 ± 0.04 mrad. It can be attributed partially to the fact that for $p < p_F$ the densities $\rho_{\Gamma M}(\boldsymbol{p}) < \rho_{\Gamma K}(\boldsymbol{p})$. Therefore, the influence of the experimental resolution function on the values of $\rho(\boldsymbol{p})$ around p_F can provide a somewhat greater displacement of $\rho(\boldsymbol{p})$ than what follows from the anisotropy of the FS. Nevertheless, the shape of the reconstructed densities suggests a greater reduction of the size of the butterflies in comparison with the band structure results. The densities $\rho(\boldsymbol{p})$ reconstructed on the succeeding planes P_i show the absence of butterflies on the planes P_3 and P_{11}. They appear between P_3 and P_4 ($p_y \simeq 1.1$ mrad) and vanish between P_{10} and P_{11} ($p_y \simeq 3.67$ mrad). This is in good agreement with both theoretical band structure calculations [12] ($p_y = 1.056$ mrad and 3.632 mrad, respectively) and results obtained by Ketterson and Stark [29] using the geometric resonance in the ultrasonic attenuation.

The influence of the e–p interaction on the e–p pair density will be discussed in the next section.

3.2. Electron–positron correlation effects in Mg

Due to the e–p interaction, the electron density at the positron site is enhanced. This problem was investigated extensively (both theoretically and experimentally) for valence electrons inside the central FS while only few papers were devoted to the enhancement of the HMC [5, 18, 34–41]. For the core electrons little is known about the momentum dependence of $\bar{\varepsilon}^c(p)$ (see [18] and references therein). For Mg, Shiotani and co-workers [11] determined a momentum independent $\bar{\varepsilon}^c(p) = 1.33$, in agreement with the theoretical value obtained by Bonderup and co-workers [42]. However, based on the former results [11] and those from references [43, 44], Šob suggested two values for γ^c of 2.24 and 1.24 for the low- and high-momentum region, respectively [45, 46], where γ^c denotes the EF for the core annihilation rate.

It has been shown in a paper [18] that the local density approach allows one to obtain not only the selective enhancement of various electronic states but also different enhancements within a given state. Due to a $r_s(\boldsymbol{r})$ dependence of $\varepsilon(\boldsymbol{r})$ (equation (5) or (6)), effective EFs for momenta $\boldsymbol{k}$ and $\boldsymbol{k} + \boldsymbol{G}$ are different (i.e. $\bar{\varepsilon}_i^v(\boldsymbol{k}) \neq \bar{\varepsilon}_i^v(\boldsymbol{k} + \boldsymbol{G})$) as well as $\bar{\varepsilon}^c(p)$ is strongly momentum dependent. In the case of valence electrons, HMC are enhanced stronger (over-enhanced) or weaker (de-enhanced) in comparison to a central FS. The other theoretical predictions [36–41] lead to the de-enhancement of the HMC contribution due to the interband transition. To our knowledge, no information about the HMC enhancement in Mg has been published until now.

We applied the approach by Daniuk and co-workers [9] described in equations (5) and (6) and obtained the anisotropic EFs for the HMC and the strongly momentum dependent EF of the core electrons.

The momentum dependence of the effective EF for the valence electrons ($\bar{\varepsilon}^v(\boldsymbol{p})$ defined in equation (2)) is presented in figure 3. Inside the FS $\bar{\varepsilon}^v(\boldsymbol{p})$ is almost isotropic and has almost the same momentum dependence as $\varepsilon(p)$, where the latter is calculated within the model of an electron gas for $r_s = 2.6$ [20]. This is due to the fact that in each point $\boldsymbol{p}$ the density $\rho(\boldsymbol{p}) \simeq \rho_i(\boldsymbol{p})$, i.e. the contribution from one of the bands dominates (it is marked in figure 3 as first, second and third band). However, due to the $\boldsymbol{r}$-dependence of $\varepsilon(\boldsymbol{r})$ there are some differences in $\bar{\varepsilon}(0)$ (see table 1). The parameter $r_s = 2.6$ corresponds to the electron density obtained theoretically at the boundary of the Wigner–Seitz cell.

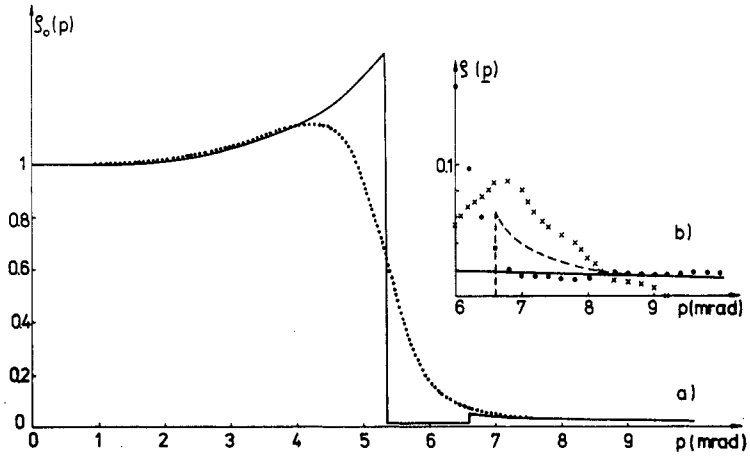

Figure 1. (*a*) The isotropic component $\rho_0(p)$ of a density on the P_1 plane reconstructed from the experimental data (dotted curve). The theoretical density $(\rho_{\Gamma M}(p) + \rho_{\Gamma K}(p))/2$ is represented by the full curve. (*b*) The densities $\rho(p)$ in the $[11\bar{2}0]$ direction obtained theoretically and by reconstruction (full curve and dotted curve, respectively). Differences between densities in $[10\bar{1}0]$ and $[11\bar{2}0]$ directions are represented by the broken curve (theory) and the crosses (reconstructed densities).

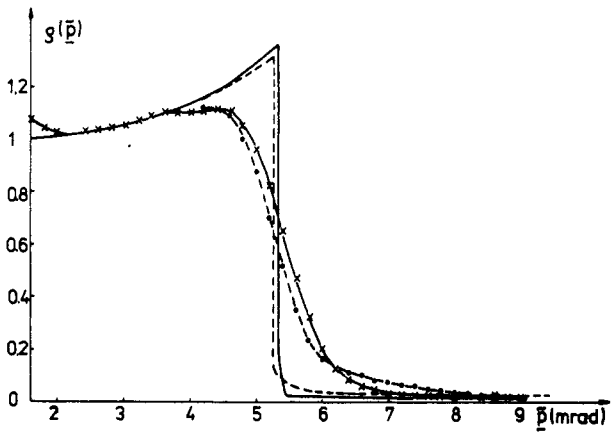

Figure 2. The densities $\rho(\underline{p})$ on the plane P_5. Full and broken curves represent the theoretical densities in $[11\bar{2}0]$ and $[10\bar{1}0]$ directions, respectively. The chain curves (— · — and — × —) show the corresponding densities obtained from the reconstruction of the 2D ACPAR data.

The shape of $\tilde{\varepsilon}^{v}(\boldsymbol{p})$ (up to $p \simeq 0.8p_F$) is in agreement with both the values extracted from the reconstructed densities and the ones found by Shiotani and co-workers [11].

In order to study the influence of $\chi_{nk}(\boldsymbol{r})$ and $r_s(\boldsymbol{r})$ on the shape of $\tilde{\varepsilon}^{v}(\boldsymbol{p})$, various enhancement functions were applied in (5). Using $\varepsilon(\boldsymbol{r})$ as $\varepsilon(0, r_s(\boldsymbol{r}))$, $\varepsilon(\sqrt{E_{nk}/E_F}, r_s(\boldsymbol{r}))$ or $\varepsilon(\sqrt{E_{nk}/E_F}, 2.6)$, the corresponding effective EFs are denoted as $\tilde{\varepsilon}^{v}_{r_s}(\boldsymbol{p})$, $\tilde{\varepsilon}^{v}_{E,r_s}(\boldsymbol{p})$ and $\varepsilon^{v}_{E}(p)$, respectively (figure 4). The application of $\varepsilon(\sqrt{E_{nk}/E_F}, r_s = 2.6)$ is equivalent to the approach proposed by Šob [47] and Mijnarends and Singru [48]. In that case

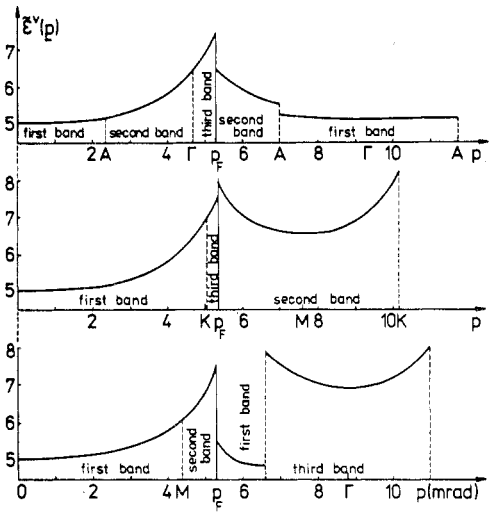

Figure 3. The momentum dependence of the effective enhancement factor $\tilde{\varepsilon}^{v}(\boldsymbol{p})$ for valence electrons of Mg in the [0001], [11$\bar{2}$0] and [10$\bar{1}$0] directions determined theoretically.

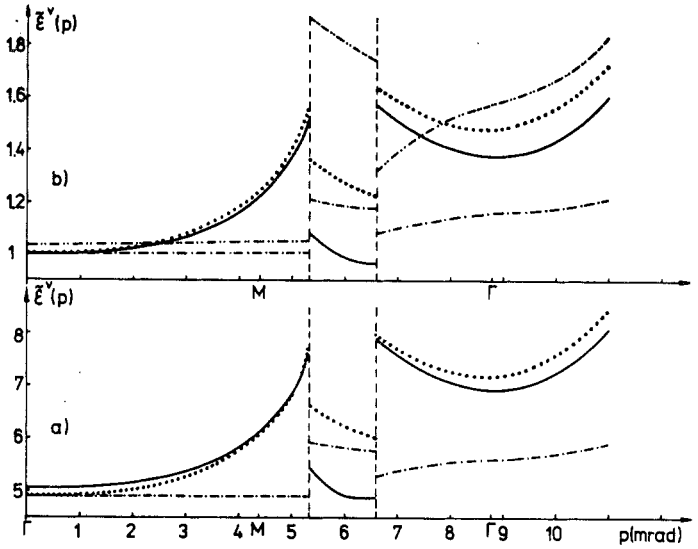

Figure 4. Effective enhancement factors for valence electrons in Mg in the [10$\bar{1}$0] direction dependent on: (*a*) $\chi_{nk}(r)$ and $r_s(r)$ (full curve), E_{nk} and $r_s(r)$ (dotted curve), $r_s(r)$ (—·—); (*b*) the same as in (*a*) but after normalization to unity. $\gamma(\boldsymbol{p})$ is represented by the curve (—··—).

$\tilde{\varepsilon}_i(\boldsymbol{k}) = \tilde{\varepsilon}_i(\boldsymbol{k} + \boldsymbol{G})$ and neither de-enhancement nor over-enhancement effects occur. If only the $r_s(\boldsymbol{r})$ dependence in $\varepsilon(\boldsymbol{r})$ is taken into account, $\tilde{\varepsilon}^{v}_{r_s}$ is constant inside the FS and equals 4.884. It is necessary to emphasize here that in the case of valence electrons, $\varepsilon(\boldsymbol{r})$ in equation (5) cannot only depend on the electron density. Such an approximation can be used in the case of positron annihilation with d or core electrons but not with valence ones, because in the former case $\tilde{\varepsilon}^{v}_{r_s}(\boldsymbol{p})$ is independent of momentum inside the FS (the same result was obtained for Na [18] and for Zn and Cd [49]). Therefore it is very

Table 1. The values of the enhancement factors for $p = 0$ ($\bar{\varepsilon}(0)$) and at the FS ($\bar{\varepsilon}(p_F)/\bar{\varepsilon}(0)$) for valence electrons in Mg. ε^{R-S} and $\bar{\varepsilon}^v(p)$, $\bar{\varepsilon}^v_{r_s}(p)$, $\bar{\varepsilon}^v_E(p)$, $\bar{\varepsilon}^v_{E,r_s}(p)$ denote free-electron gas EF for $r_s = 2.6$ [20] and the effective EF obtained from equation (5) for $\varepsilon(r) = \varepsilon(\chi_{nk}(r), r_s(r))$, $\varepsilon(r) = \varepsilon(0, r_s(r))$, $\varepsilon(r) = \varepsilon(\sqrt{E_{nk}/E_F}, 2.6)$ and $\varepsilon(r) = \varepsilon(\sqrt{E_{nk}/E_F}, r_s(r))$, respectively.

	$\varepsilon^{R-S}_{r_s=2.6}$	$\bar{\varepsilon}^v$	$\bar{\varepsilon}^v_{r_s}$	$\bar{\varepsilon}^v_E$	$\bar{\varepsilon}^v_{E,r_s}$
$\bar{\varepsilon}(0)$	5.12	5.044	4.884	5.12	4.884
$\bar{\varepsilon}(p_F)/\bar{\varepsilon}(0)$	1.54	1.51	1.01	1.54	1.55

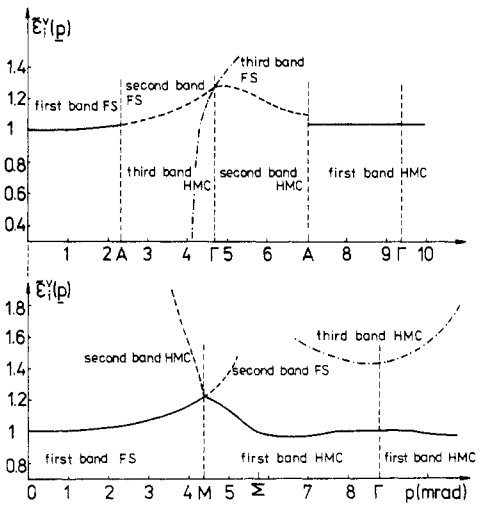

Figure 5. The momentum dependence of the partial enhancement factors $\bar{\varepsilon}^v_i(p)$ for an ith band along the [0001] and [01$\bar{1}$0] directions.

important to take into account the momentum (or energy) dependence of $\varepsilon(r)$ in equation (5).

Inside the FS, $\bar{\varepsilon}^v_{r_s}(p)$ is a constant, while it is strongly momentum dependent and anisotropic in a region of HMCs. Such an effect is not unexpected when one compares the shape of $\bar{\varepsilon}^v_{r_s}(p)$ with a function $\gamma(p) = \rho^{IPM}(p)/\rho_e(p)$, where ρ_e denotes an electron density at the absence of the positron. If multiplication of $\Psi_{nk}(r)$ by $\Psi_+(r)$ provides an anisotropic and momentum dependent $\gamma(p)$ function, the enhancement (which depends on the electron density at various lattice points) should provide similar effects (see also [18]). As a result the over-enhancement ($\bar{\varepsilon}^v_i(k + G) > \bar{\varepsilon}^v_i(k)$) or de-enhancement ($\bar{\varepsilon}^v_i(k + G) < \bar{\varepsilon}^v_i(k)$) can be obtained. It can be seen from figure 5 that in the ΓA direction the HMC contribution of the 3rd band for $p < |2\Gamma A|$ is strongly de-enhanced. However, in this region $\rho^{IPM}(p) \simeq \rho^{IPM}_2(p)$ and this de-enhancement does not influence the shape of the effective EF $\bar{\varepsilon}^v(p)$ (compare figure 3 and figure 5). In the ΓM direction the HMC contribution from the 3rd band is over-enhanced (figure 5). Since in this region $\rho^{IPM}(p) \simeq \rho^{IPM}_3(p)$, we have $\bar{\varepsilon}^v(p) \simeq \bar{\varepsilon}_3(p)$ (figure 3). Moreover, because the contribution of this band is relatively high, this over-enhancement (if it exists) should be observable by experiment. This effect is clearly visible from the reconstructed densities as discussed in the previous section.

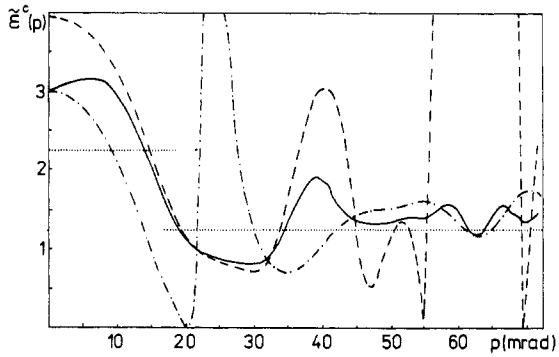

Figure 6. The momentum dependence of the theoretical effective enhancement factor $\tilde{\varepsilon}^c(p)$ for core electrons in Mg (full curve). The broken and chain curves represent EFs for the 2p and 2s states, respectively. The dotted lines correspond to values of λ^c in the low- and high-momentum regions found in [46].

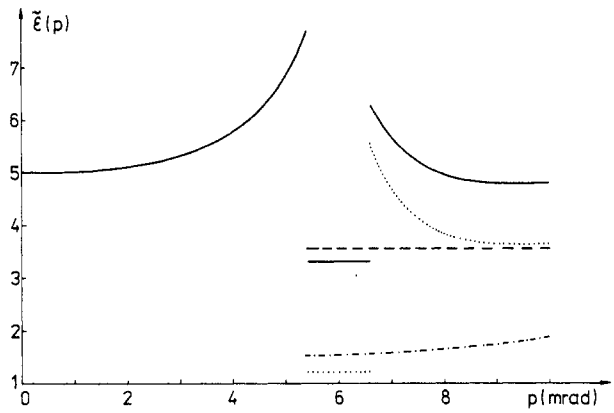

Figure 7. The theoretical effective enhancement factor $\tilde{\varepsilon}(\boldsymbol{p})$ for the total density. Full and broken curves describe the EF in the ΓM and ΓK directions, respectively, when the e–p interaction was taken into account for both the valence and core electrons. The dotted and chain curves show the corresponding $\tilde{\varepsilon}(\boldsymbol{p})$ when the core contribution was calculated within the IPM.

Figure 6 shows the theoretical EF of core electrons in Mg. The reason why oscillations of $\tilde{\varepsilon}_i^c(p)$ appear in a region of higher momenta is discussed in [18]. The dependence of $\varepsilon^c(p)$ is consistent with the behaviour of low- (2.24) and high-momentum (1.24) values of γ^c found in [46]. However, the EF γ^c following from our theoretical results is slightly higher and equals 2.44, although somewhat lower than $\lambda^c = 2.59$ obtained by Jensen [50]. The comparison of the theoretical densities with the reconstructed ones indicates that these surprisingly high values of $\tilde{\varepsilon}^c(p)$ ($\tilde{\varepsilon}^c(p) \simeq 3.2$ for $p < 10$ mrad) with respect to $\tilde{\varepsilon}^v(0) = 5.044$ are really observed in the experiment.

The total theoretical effective EF (defined in equation (2)) along the ΓK and ΓM direction is presented in figure 7 for the cases when $\tilde{\varepsilon}^c \neq 1$ (as in figure 6) and for $\varepsilon^c = 1$. Generally, the shape of $\tilde{\varepsilon}(\boldsymbol{p})$ depends not only on $\tilde{\varepsilon}^v$ (or $\tilde{\varepsilon}_i^v$) and $\tilde{\varepsilon}^c$ but also on a

momentum dependence of $\rho_v^{IPM}(\boldsymbol{p})$ and $\rho_c^{IPM}(\boldsymbol{p})$. Such an effect is observed in the ΓM direction where the shape of $\rho_3^{IPM}(\boldsymbol{p})$ influences the shape of $\tilde{\varepsilon}(\boldsymbol{p})$ for $p \geq 6.6$ mrad. This picture shows that it is impossible to extract information about the enhancement of the separate electronic states if only the two functions $\rho(\boldsymbol{p})$ and $\rho^{IPM}(\boldsymbol{p})$ are known, the first determined from experiment and the second theoretically.

4. Conclusions

(i) The reconstruction of the 2D ACPAR experimental spectra in Mg [6] shows the anisotropy of the FS: the butterflies and fourth-zone electron pockets around L and holes around H are decreased. The dimension of butterflies along the [0001] direction is in agreement with the theoretical [12] and experimental [29] band structure results. However, their decrease along lines parallel to ΓM is about two times greater than in theory.

(ii) The disagreement between the IPM theory and experiment was much reduced by introducing the e–p correlations in the local density approximation [9].

(iii) The shape of the theoretical EF $(\tilde{\varepsilon}^v(p)/\tilde{\varepsilon}^v(0))$ inside the FS in Mg does not differ essentially from a free-electron gas EF for $r_s = 2.6$ [20]. However, its value for $p = 0$ $(\tilde{\varepsilon}^v(0))$ depends on the effective electron density. So, the local density treatment is important in determining relative contributions to $\rho(\boldsymbol{p})$ from various electronic states as well as for the interpretation of the total annihilation rates.

(iv) The local density equation (5) leads to an over-enhancement or de-enhancement of HMC. It seems that the reconstructed densities confirm the effect of the over-enhancement obtained theoretically for HMC of the third band in the ΓM direction.

(v) The theoretical calculations provide evidence for a strongly momentum-dependent EF for core electrons in Mg. Comparison with the reconstructed densities in the ΓK direction (where the contribution of HMC is negligible) confirms the high values of $\tilde{\varepsilon}^c(p)$ for momenta $p < 10$ mrad (3.2 in comparison with $\tilde{\varepsilon}^v(p = 0) = 5.044$ in the case of valence electrons). It is also in good agreement with the results for the total core annihilation rate [46, 51].

(vi) The idea of introducing into the integral contained in the definition of $\rho(\boldsymbol{p})$ (equation (5)) the EF depending on the local density and the local kinetic energy is due to Daniuk and co-workers [9]. Since then there were various attempts at modifying the position dependence of the EF by neglecting the dependence on the kinetic energy [18, 24, 52]. These attempts can lead, of course, to a limited success, especially, if the effective EF is not well described by the jellium results [53, 54]. In the case of valence electrons the EF in (5) cannot depend only on the electron density. Such a treatment leads to a momentum-independent effective EF $(\tilde{\varepsilon}^v(p))$ inside the FS. The momentum dependence of $\tilde{\varepsilon}^v(\boldsymbol{p})$ has been found beyond doubt in most metals, e.g. in Mg in the present work.

Acknowledgments

We are grateful to Dr P A Walters, Dr J Mayers and Professor R N West for providing the experimental 2D ACPAR spectra for Mg and to Dr A Rubaszek, Dr M Šob and Professor H Stachowiak for helpful discussions.

References

[1] Brandt W and Dupasquier A (eds) 1983 *Positron Solid-State* (Amsterdam: North-Holland)
[2] Hautojärvi P (ed) 1979 *Positrons in Solids* (Heidelberg: Springer)
[3] Majumdar C K 1965 *Phys. Rev.* A **140** 227
[4] Kubica P and Stewart A T 1975 *Phys. Rev. Lett.* **34** 852
[5] Kontrym-Sznajd G and Šob M 1988 *J. Phys. F: Met. Phys.* **18** 1317
[6] Walters P A, Mayers J and West R N 1982 *Positron Annihilation* eds P G Coleman, S C Sharma and L M Diana (Amsterdam: North-Holland) p 334
[7] Cormack A M 1964 *J. Appl. Phys.* **35** 2908
[8] (a) Kontrym-Sznajd G 1982 *Positron Annihilation* eds P G Coleman, S C Sharma and L M Diana (Amsterdam: North-Holland) p 346
(b) ——1989 *Solid State Commun.* **70** 1011
(c) ——1990 *Phys. Status Solidi* a **117** 227
[9] Daniuk S, Kontrym-Sznajd G, Mayers J, Rubaszek A, Stachowiak H, Walters P A and West R N 1985 *Positron Annihilation* eds P C Jain, R M Singru and K P Gopinathan (Singapore: World Scientific) p 254; 1987 *J. Phys. F: Met. Phys.* **17** 1365
[10] Becker E H, Senicki E M D, Gould A G and Hogg B G 1972 *Can. J. Phys.* **50** 2520
[11] Shiotani N, Okada T, Sekizawa H and Wakoh S 1981 *J. Phys. Soc. Japan* **50** 498
[12] Daniuk S, Jarlborg T, Kontrym-Sznajd G, Majsnerowski J and Stachowiak H 1989 *J. Phys.: Condens. Matter* **1** 6321
[13] Anderson O K 1975 *Phys. Rev.* B **12** 3060
[14] Jarlborg T and Arbman G 1976 *J. Phys. F: Met. Phys.* **6** 189
[15] Skriver H L 1984 *The LMTO Method* (Heidelberg: Springer)
[16] Hedin L, Lundqvist B I and Lundqvist S 1971 *Solid State Commun.* **9** 537
[17] Singh A K and Jarlborg T 1985 *J. Phys. F: Met. Phys.* **15** 727
[18] Daniuk S, Kontrym-Sznajd G, Majsnerowski J, Šob M and Stachowiak H 1989 *J. Phys.: Condens. Matter* **1** 6321
[19] Rubaszek A, Stachowiak H, Boroński E and Szotek Z 1984 *Phys. Rev.* B **30** 2490
[20] Rubaszek A and Stachowiak H 1984 *Phys. Status Solidi* b **124** 159
[21] Lowy D N and Jackson A D 1975 *Phys. Rev.* B **12** 1689
[22] Arponen J and Pajanne E 1979 *J. Phys. F: Met. Phys.* **9** 2359
[23] Lowy D N 1982 *Phys. Rev.* B **26** 60
[24] Jarlborg T and Singh A K 1987 *Phys. Rev.* B **36** 4660
[25] Singh A K, Manuel A A, Jarlborg T, Mathys Y, Walker E and Peter M 1986 *Helv. Phys. Acta* **59** 410
[26] Daniuk S 1989 *J. Phys.: Condens. Matter* **1** 5561
[27] Cormack A M 1973 *Phys. Med. Biol.* **18** 195
[28] Kontrym-Sznajd G and Majsnerowski J 1989 *Solid State Commun.* **70** 593
[29] Ketterson J B and Stark R W 1967 *Phys. Rev.* **156** 748
[30] Wakoh S 1981 *J. Phys. Soc. Japan* **50** 490
[31] Rozenfeld B and Chabik S 1977 *Appl. Phys.* **13** 81
[32] Brandt W, Eder L and Lundqvist S 1966 *Phys. Rev.* **142** 165
[33] Mijnarendes P E 1979 *Positrons in Solids* ed P Hautojärvi (Heidelberg: Springer) p 25
[34] Oberli L, Manuel A A, Sachot R, Descouts P and Peter M 1985 *Phys. Rev.* B **31** 6104
[35] Hede B B J and Carbotte J P 1972 *J. Phys. Chem. Solids* **33** 727
[36] Fujiwara K, Hyodo T and Ohyma J 1972 *J. Phys. Soc. Japan* **33** 1047
[37] Sormann H, Nowak P, Kindl P and Puff W 1982 *Positron Annihilation* eds P G Coleman, S C Sharma and L M Diana (Amsterdam: North-Holland) p 218
[38] Sormann H and Puff W 1985 *Positron Annihilation* eds P C Jain, R M Singru and K P Gopinathan (Singapore: World Scientific) p 161
[39] Sormann H 1987 *Thesis (Habilitationsschrift)* Technische Universität, Graz
[40] Sormann H 1987 *Phys. Status Solidi* b **142** K45
[41] Sormann H 1989 *Positron Annihilation* eds L Dorikens-Vanpreat, M Dorikens and D Segers (Singapore: World Scientific) p 37
[42] Bonderup E, Anderson J U and Lowy D N 1979 *Phys. Rev.* B **20** 883
[43] Maninen M, Nieminen R and Hautojärvi P 1975 *Phys. Rev.* B **12** 4012
[44] Kubica P and Stewart A T 1983 *Can. J. Phys.* **61** 971
[45] Šob M 1985 *Solid State Commun.* **53** 249

[46] Šob M 1985 *Solid State Commun.* **53** 255
[47] Šob M 1978 *Proc. 8th Ann. Int. Symp. on Electronic Structure of Metals and Alloys* ed P Ziesche (Dresden: Technische Universität) p 170; see also Šob M 1982 *J. Phys. F: Met. Phys.* **12** 571
[48] Mijnarends P E and Singru R M 1979 *Phys. Rev.* B **19** 6038
[49] Kontrym-Sznajd G and Majsnerowski J (in preparation)
[50] Jensen K O 1989 *J. Phys.: Condens. Matter.* **1** 10595
[51] Johnson O 1980 *Phys. Status Solidi* b **99** 745
[52] Rubaszek A 1989 *J. Phys.: Condens. Matter.* **1** 2141
[53] Rubaszek A and Stachowiak H 1988 *Phys. Rev.* B **38** 3846
[54] Stachowiak H 1990 *Phys. Rev.* B **41** 12522